16th World Conference on Earthquake, 16WCEE 2017

Santiago Chile, January 9th to 13th 2017

Paper N° 105

Registration Code: S-XXXXXXXX

EARTHQUAKE-INDUCED FLOOR ACCELERATIONS IN BASE ISOLATED STRUCTURES

P.M. Calvi[(1)], D.M. Ruggiero[(2)]

[(1)] *Assistant Professor, Department of Civil and Environmental Engineering, University of Washington, Seattle, WA, USA, pmc85@uw.edu*

[(2)] *Postdoctoral Researcher, IUSS - Istituto Universitario di Studi Superiori di Pavia, Pavia, PV, Italy, david.ruggiero@iusspavia.it*

Abstract

In order to meet desired seismic performances, it is increasingly evident that engineers require reliable methods for the estimation of seismic demands on both structural and non-structural elements. To this end, current design codes incorporate simplified methods for the prediction of acceleration demands on secondary structural and non-structural elements for buildings with fixed bases. However, no guidance is currently provided as to how to estimate the seismic demand on non-structural elements in base isolated structures. In such structures, large floor accelerations may still be recorded, particularly in the case of higher mode interactions or horizontal-vertical coupling effects. In all cases, determining the seismic demand on non-structural elements is necessary in order to be able to perform a rational design of those elements, and to be able to effectively control their seismic response.

In order to take a step towards the formation of accurate yet simplified methods of predicting peak floor accelerations and floor spectra in base isolated structures, this analytical work examines the response of a number of base isolated case study structures subjected to a series of ground motions of varying intensity. The results of the non-linear time history analyses are used to identify the factors that appear to affect the shape and intensity of acceleration demands on secondary structural and non-structural elements.

Keywords: floor acceleration spectra; base isolation; performance-based design; nonlinear time history analysis

1. Introduction

Earthquakes are amongst the deadliest and most costly natural catastrophes that affect society. Over the years, earthquakes have been the cause of thousands of casualties and of very high financial losses. In the US alone, the annual earthquake losses are estimated at $4.4B (FEMA, 2008).

Seismic events such as the Darfield (New Zealand) earthquake of September 2010 (Dhakal 2010) and the Northridge (USA) earthquake of 1994 (Villaverde 1997) have demonstrated that even though modern seismic design techniques can successfully limit damage to main structural elements during intense shaking, the damage to secondary structural and non-structural elements may be extensive, very costly and in some cases even life threatening. In the M7.1 Darfield earthquake, which imposed seismic demands similar to the design code level for the ultimate limit state in the Christchurch region, total losses have been estimated at NZ$5 billion (The Treasury, Government of New Zealand 2011) even though there was no loss of life. More details on non-structural damage related issues in recent earthquakes can be found in the work of Filiatrault and Sullivan (2014).

Given its emerging importance, the seismic vulnerability of non-structural elements has been the object of numerous investigations and, particularly in the last half century, much effort has been devoted to developing rational methods for quantifying the seismic demand and conducting the analysis of non-structural elements. In general, the performance of non-structural elements tends to be dependent on storey drift demands, acceleration demands or both. While non-structural drift limits can typically be incorporated directly into the structural design procedure, acceleration-sensitive elements require further analysis. Techniques have been proposed for generating floor acceleration spectra to aid in the design and analysis of acceleration-sensitive elements such as suspended ceiling systems and mechanical equipment anchored to a single building level; as research has shown that the seismic demand on such elements can be quite high.

When it is impractical to limit the floor accelerations in a structure using traditional lateral load resisting systems, designers may choose to turn to base isolation instead. In recent years many base isolation solutions have been developed for practical use, and they have proven to be effective in ensuring a high level of structural performance under earthquake-induced lateral loads. Therefore, one might expect that isolation would provide protection for acceleration-sensitive non-structural elements as well. However, the results of two recent test programs on full scale isolated buildings conducted at the National Institute for Earth Science and Disaster Prevention (NIED) E-Defense shaking table of Japan (Warn and Ryan 2012; Ryan et al., 2012) have shown that the elastomeric and the friction isolation systems considered could only guarantee the functionality of the structure in case of a near-fault motion but not for a long duration, long period ground motion generated from a subduction earthquake. In general, large accelerations were recorded at the various levels of the base isolated structures and significant damage to the non-structural elements was observed.

While extensive literature is available on floor accelerations in traditional fixed-base structures, investigations into floor accelerations in isolated structures are very limited. Furthermore, in contrast with traditional structures, no approximate approaches or code provisions are currently available for constructing floor response spectra for base isolated structures.

In light of these observations, this analytical work is intended to provide some insight into the seismic demand on non-structural elements in base isolated structures. Results of non-linear time history analyses (NLTHAs) of different case-study structures will be used to illustrate the factors that influence floor accelerations in structures isolated using friction pendulum (FP) systems.

2. NLTHA of case study base isolated structures

In order to investigate the floor accelerations in base isolated structures, a series of three case-study buildings of different heights have been designed and subjected to lateral excitation. This section presents the analyses in three sections: firstly, the design of the representative base isolated structures is described; secondly, details of the NLTH modelling and analysis approach are provided; and finally, the resulting floor acceleration spectra for each of the structures are reported and compared to the spectra provided by code approaches for traditional structures.

2.1 Description of the case study base isolated structures

The design of three realistic base isolated case study structures has been performed using a displacement-based methodology. The three structures correspond to 4-, 8-, and 12-storey reinforced concrete frames, so as to provide a range of natural periods, and it has been assumed that isolation will be provided in the form of FP devices. The structures are modelled as multiple degree-of-freedom (MDOF) shear systems with lateral displacement degrees-of-freedom at each level. The storey weight was taken as 3000 kN, while the storey height was assumed to be 2.8 m, with an additional 0.2 m for the isolation level. For the seismic input, a design spectrum with a corner period of 4 s and a corresponding maximum spectral displacement of 0.9 m has been assumed.

The displacement-based design (DBD) procedure is based on the recommendations of Priestley, Calvi and Kowalsky (2007) and is briefly summarized below. In general, direct DBD is performed by assuming the design displacement profile of a structure, calculating the equivalent single degree-of-freedom (SDOF) properties of the system, and using a damping-corrected displacement spectrum to determine the necessary strength and stiffness to achieve the desired displacement.

DBD for isolated structures may be performed in a similar manner. The design displacement is taken as the sum of the displacement in the isolation level and the displacement of the superstructure. Since the base isolation is intended to keep the superstructure from yielding, only the elastic displacements of the frame need to be considered. In calculating the SDOF properties for a FP system there is the additional complexity that the equivalent damping of the device depends on two parameters: the radius of curvature of the bearing and its friction coefficient. The design procedure is therefore iterative and open-ended; many combinations of curvature and friction may satisfy the same design requirements. For this reason it can be easier to invert the problem; that is, to begin with realistic parameters for the FP and iteratively calculate the maximum displacement expected. The parameters are then updated until the desired displacement is achieved.

The iterative design procedure is summarized in Fig. 1. For purposes of the calculation, it has been assumed that the yield strain of the reinforcing steel ε_y is 0.002, that the length of the beams L_b is 5 m, and that the depth of the beams h_b is 0.8 m.

(1) Initialization

Given: friction μ; radius of curvature R; structure weight W

Guess: isolator displacement $\Delta_{d,iso}$.

(2) Displacement profile

$$\Delta_{d,sys} = \Delta_{d,iso} + \Delta_{d,es}$$

$$\Delta_{d,es} = H_e \cdot \theta_y$$

$$\theta_y = 0.5 \cdot \varepsilon_y \cdot \frac{L_b}{h_b} \quad \text{(Priestley et al. 2007)}$$

(3) Effective SDOF properties (Chopra 2000)

$$H_e = \frac{\sum_i m_i \Delta_i H_i}{\sum_i m_i \Delta_i}$$

$$m_e = \frac{\sum_i m_i \Delta_i}{\Delta_{d,sys}}$$

$$T_e = \sqrt{4\pi^2 \cdot \frac{m_e \cdot \Delta_{d,sys}}{V_b}}$$

$$V_b = W \cdot \mu + \frac{W}{R} \cdot \Delta_{d,iso}$$

(4) Equivalent viscous damping

$$\xi_{e,iso} = \frac{1}{2\pi} \cdot \frac{A_{hyst}}{V_b \cdot \Delta_{d,iso}} \quad \text{(Jacobsen 1960)}$$

$$A_{hyst} = 4 \cdot W \cdot \mu \cdot \Delta_{d,iso}$$

$$\xi_{e,sys} = \frac{\xi_{e,es}\Delta_{d,es} + \xi_{e,iso}\Delta_{d,iso}}{\Delta_{d,sys}}$$

(5) Displacement spectrum

$$\eta = \sqrt{\frac{0.07}{0.02 + \xi_{e,sys}}} \quad \text{(Priestley et al. 2007)}$$

$$\Delta^*_{d,sys} = \eta \Delta_{T_c} \cdot \frac{T_e}{T_c}$$

(6) Revise isolator displacement and iterate

$$\Delta^*_{d,iso} = \Delta^*_{d,sys} - \Delta_{d,es}$$

Fig. 1 – Design procedure for base isolation of a multi-storey structure (after Priestley, Calvi & Kowalsky, 2007)

Repeating the process for many combinations of friction and radius curvature, one can generate a "map" of possible structural responses to the imposed ground motion. This is visualized in Fig. 2 for the 4-storey structure. Maps for the 8- and 12- storey structures are similar in form, however the displacement and shear ordinates differ.

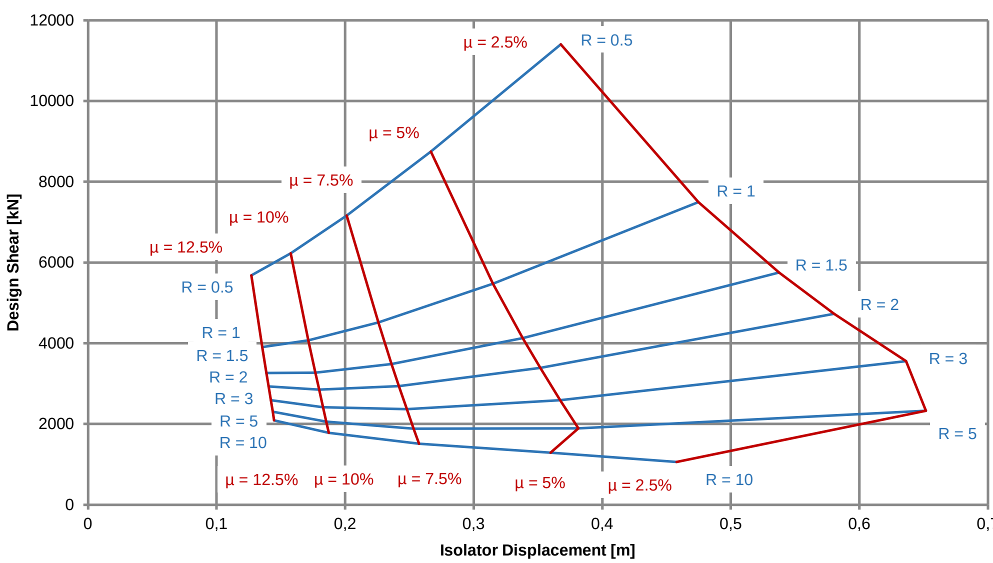

Fig. 2 – Base isolation system design map for the 4-storey case study structure

As desired, this two-variable map allows the designer to select the physical properties (friction and radius) of the FP required to achieve a certain displacement and force. Alternatively, it affords the designer the option of

imposing constraints such as manufacturability of different devices. Furthermore, it makes clear some of the bounds of this isolation scheme; for example, it is apparent that using a friction coefficient higher than 5% always results in a displacement lower than 400 mm independent of the radius of curvature of the device.
For the present study, the isolator displacement has been set to a maximum of 400 mm, and the selection of the FPs has been limited to industrially available devices; a viable solution is to use a radius of curvature of 3.7 m and a friction coefficient of 5.5% for each of the buildings.
In order to model the elastic stiffness of the superstructure as equivalent shear springs, it is assumed that the base shear is distributed to the structure in proportion to the mass and displacement; that is, according to the elastic mode shape. This allows for the calculation of storey shears and the equivalent stiffness of each storey based upon the yield drift previously assumed:

$$K_{es,i} = \frac{V_i}{\Delta_i - \Delta_{i-1}} \tag{1}$$

where the subscript i represents the storey number.
Using these storey stiffnesses and the hysteretic properties of the isolator, it is possible to construct a MDOF non-linear model for each of the case study structures (Fig. 3).

2.2 Non-linear time-history modeling and analysis approach

A customised computer program was written in Matlab (Matlab 2012) to compute the non-linear dynamic response of base isolated structures to base excitations. The program solves the incremental equation of motion using a linear acceleration Newmark-Beta integration algorithm (Newmark and Rosenblueth 1971) and can perform the analysis of non-linear MDOF "shear-type" structures, such as that idealized in Fig 3 (a). The isolation system is simulated using a non-linear translational spring characterized by an appropriate relationship between lateral force and displacement. The hysteresis of this spring is defined as a function of the isolator selected (i.e. the friction pendulum for the present study). The structure is idealized as a series of masses connected by translational springs that can be assigned linear or non-linear (elastoplastic, with or without hardening) hysteretic behavior. In this context, the masses are lumped at the floor levels and are allowed to translate exclusively in the x-direction.

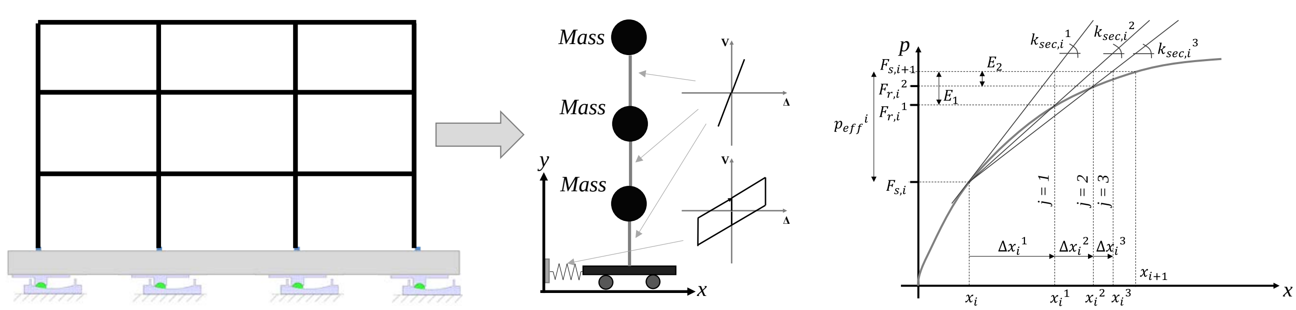

(a) Schematic of structural model. (b) Calculation of the secant stiffness.

Fig. 3 – Modeling idealizations considered by the program

The damping matrix is obtained as a function of both the stiffness and the mass matrices, adopting an initial stiffness proportional Rayleigh model and assigning a low damping ratio to modes 1 and (n – 1), where n is the number of stories (ξ = 1%, as suggested by Pant et al. 2013). To this end, the fundamental mode of the structure is computed in the program based on the initial stiffness of the isolation system (i.e. before the isolation system is activated). The choice of using Rayleigh damping was principally dictated by computational concerns, and it was considered satisfactory on account of the preliminary nature of this work. However, to deal with more complex structures, it may be necessary to incorporate alternative damping models as the Rayleigh model tends to produce unrealistically high damping of lower frequencies (Petrini et al. 2008; Smyrou at al. 2011) leading to overly optimistic predictions of the performance of base isolated structures (Hall 2006, Ryan and Polanco, 2008).

To minimize the occurrence of numerical errors, the instantaneous stiffness of the system is evaluated iteratively within each time step. This is done by employing an iterative procedure of the Newton-Raphson family, as summarized in Fig 3 (b).

The numerical simulations were run using a set of 7 real ground motions as input. The records were selected to be compatible with the displacement design spectrum used previously; that is, with a corner period at 4 seconds corresponding to a displacement of 0.9 meters for a damping ratio of 5%.

In the selection process, a preliminary screening was performed to limit the search to records pertaining to soil type A (i.e. essentially on firm rock) and whose closest distance to the fault was in a range of 20 to 120 km. The limits on distance aimed to avoid near-fault effects and excessive attenuations of the records. The ground motions were appropriately scaled so that the average displacement spectrum associated to the motions matched the selected displacement design spectrum. The key characteristics of the 7 records selected are summarized in Table 1. For more information the reader is invited to refer to the work of Fagà (2013).

Table 1 – Characteristics of the records of the ground motion set

ID	PEER ID	EQ Name	Magnitude M_w	Clst. Dist. [km]	SF
EQ1	2107	Denali, Alaska	7.9	51	9.35
EQ 2	1446	Chi-Chi, Taiwan	7.6	119	17.75
EQ 3	1440	Chi-Chi, Taiwan	7.6	122	6.56
EQ 4	-	Darfield	7.1	130	7.11
EQ 5	-	Darfield	7.1	51	22.69
EQ6	284	Irpinia-01	6.9	10	7.58
EQ7	1074	Northridge-01	6.7	42	13.04

The displacement and acceleration response spectra associated to each ground motion, the average spectra and the design spectra are shown in Fig. 4. It can be seen that the average displacement spectrum lies reasonably close to the target (design) spectrum, while the individual curves, in some instances, diverge from the average.

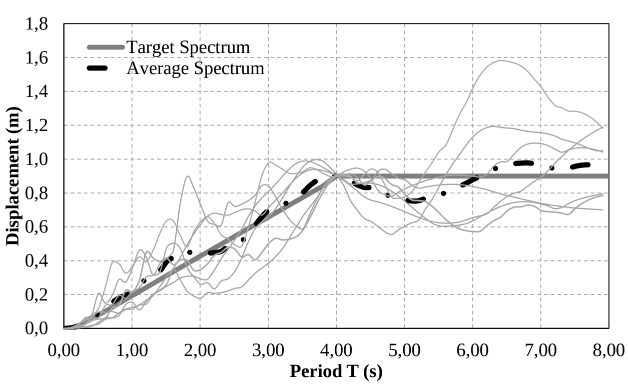

(a) Displacement response spectra

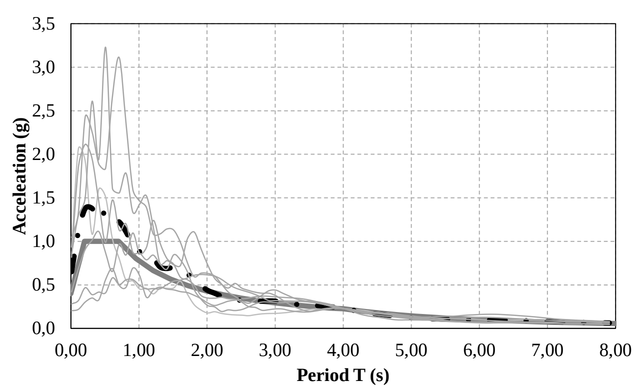

(b) Acceleration response spectra

Fig. 4 – Response spectra for non-linear time history analyses

2.3 Floor response spectra obtained from the NLTH analyses

Floor response spectra were obtained by first extracting the acceleration time history recorded at the various building levels during the NLTHAs and then using numerical techniques (see Chopra 2000) to calculate the corresponding acceleration response spectra. In this way, floor-level response spectra were generated at each storey level following each NLTHA.

Since floor response spectra can be constructed for different values of elastic damping that the non-structural elements might be assumed to possess, 2%, 5%, 10% and 20% damped spectra were developed in this phase of the research. Fig. 5 presents the average ground floor, mid-height and roof level spectra obtained for the three case-study structures.

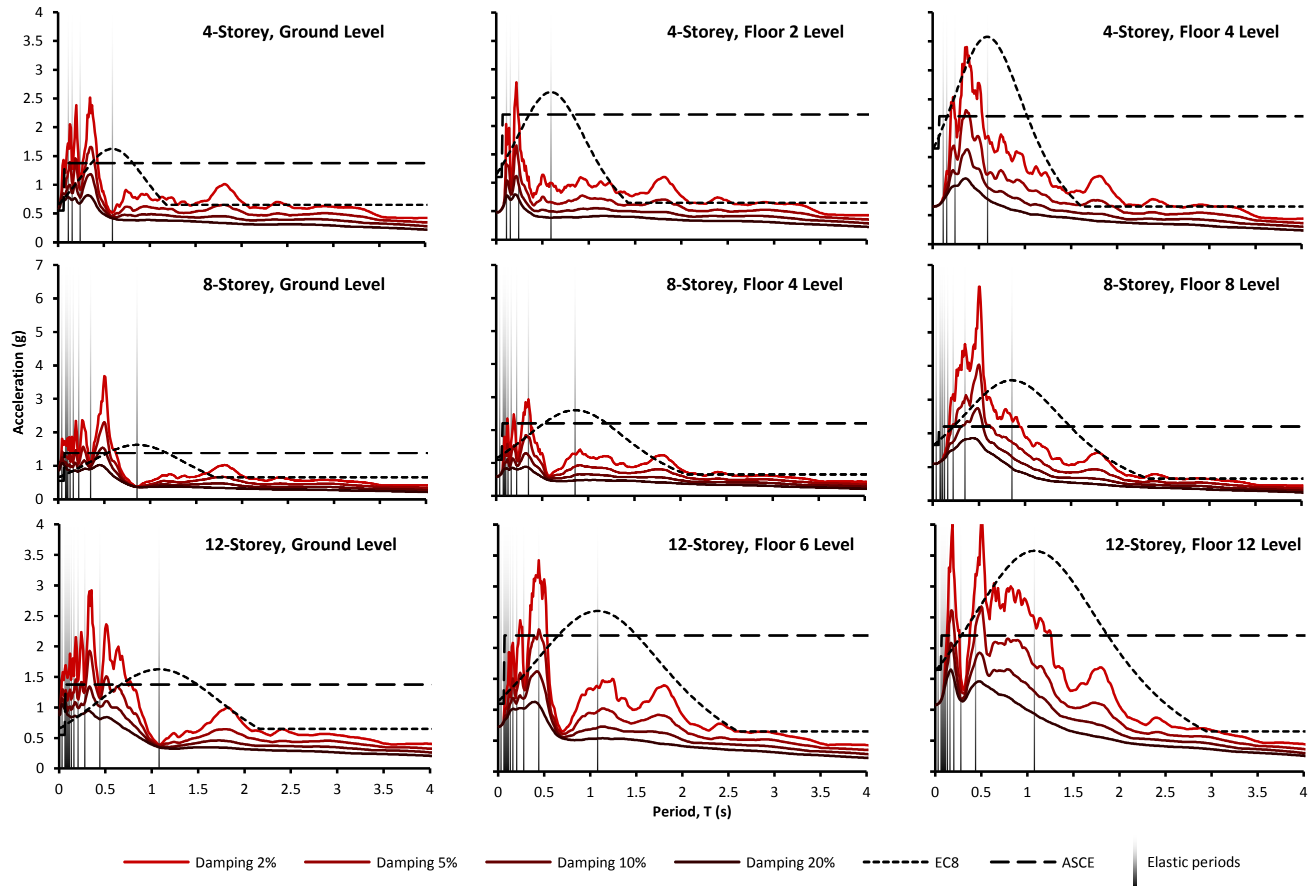

Fig. 5 – Comparison of ground floor, mid-height and roof level response spectra predicted via code approaches and via NLTHA of the case study structures subjected to ground motions compatible with the design spectrum

The floor response spectra obtained from the numerical analyses are compared with the predictions obtained in line with the recommendations currently in effect in Europe and in the USA to deal with non-isolated structures. More specifically, the two codes considered were the Eurocode 8 (CEN EC8 2004) and the ASCE 7-10.

In the Eurocode 8 the acceleration demand, S_a, acting on a non-structural element of a building can be obtained from

$$S_a = a_g \cdot S \cdot \left(\frac{3(1+z/H)}{1+(1-T_a/T_n)^2} - 0.5 \right) \geq a_g \cdot S \qquad (2)$$

where a_g is the design ground acceleration (in units of g) for a rock site, S is a modification factor to account for other soil site conditions, z is the height of the non-structural element above the ground level, H is the total height of the building, T_a is the period of the non-structural element and T_n (denoted T_1 in Eurocode 8) is the natural (first-mode) period of the building in the relevant direction of excitation.

At roof level, Eq. (2) suggests that the peak elastic acceleration imposed on a non-structural element (obtained when $Ta = T1$) will be 5.5 times the peak ground acceleration (PGA) at the site.

According to ASCE 7-10, the horizontal acceleration to be applied at the component's center of gravity and distributed relative to the component's mass is given by:

$$S_{ah} = \frac{0.4 \cdot a_p \cdot S_{DS}}{\left(\frac{R_p}{I_p}\right)} \cdot \left(1 + 2\frac{z}{h} - 0.5\right) \tag{3}$$

where a_p is the component amplification factor; S_{DS} is the design earthquake spectral response acceleration at short period (0.2 s); R_p is the component response modification factor; I_p is the component importance factor; z is the height of the structure at point of attachment of the non-structural component and h is the average roof height of structure relative to the base elevation. Furthermore, the horizontal design accelerations must satisfy the following minimum and maximum values.

$$0.3 \cdot S_{DS} \cdot I_p \leq S_{ah} \leq 1.6 \cdot S_{DS} \cdot I_p \tag{4}$$

In the present work, for both cases, the most conservative situation has been adopted to establish equivalent acceleration demands for predictions in Fig. 5.

A number of important observations can be made from Fig. 5. Firstly, one may note that the spectral demands predicted by the international codes tend to underestimate, somewhat unexpectedly, the peak acceleration demands in all cases. At the same time, the ASCE 7-10 predictions significantly overestimate the demand on flexible non-structural elements (e.g. T > 0.5 s).

The second point to note is that the accelerations are significantly affected by the damping ratio selected for the construction of the spectra. For example, accelerations at 2% damping are approximately 50% higher than those at 5% damping. It is evident that spectral acceleration demands depend on the damping of the non-structural elements and that this parameter should be accounted for. In fact, none of the international codes appear to take into account the likely elastic damping of the non-structural elements when estimating the acceleration demands. However, it is interesting to note in Fig. 5 that for non-structural elements characterized by certain periods of vibration, the damping ratio appears to have almost no influence. Notably, in all three cases at the ground level there is a valley corresponding to the fundamental period. It is possible that these valleys correspond to fixed nodes in the dynamic response of the structures.

Thirdly, for cases with relevant effects induced by the higher modes, it is possible to observe acceleration spikes corresponding to the higher periods that neither code approach is able to capture. In the case of EC8, only acceleration amplification associated with the fundamental period of vibration is considered; it is evident from Fig. 5 that, even for base isolated structures, floor spectra can be significantly affected by higher modes (i.e. lower periods). Furthermore, the EC8 also misses the peaks at longer periods as it does not capture period elongations due to the activation of the base isolators and to the effects of non-linearity, as discussed in more detail in the next sections. In the case of ASCE, essentially no distinction is made for non-structural elements of different fundamental periods, and therefore this approach tends to underestimate demands for short period elements and overestimate demands for long period elements.

In summary, it has been demonstrated that floor response spectra predicted according to the code provisions available for traditional structures are not accurate for base isolated structures. In light of these results, the remainder of this paper will focus on understanding the reasons for these discrepancies. Future research should look in more detail into developing simplified approaches that can be used to predict floor spectra at the various levels of a base isolated structure.

3. Interpreting the results: what influences floor spectra in base isolated structures?

3.1 Effects of damping

While values of the elastic damping of secondary structural and non-structural elements should be an area for future research, one could certainly expect values to range from around 1% to 2% for systems such as glass façade systems (Nakagami 2003, Lenk and Coult 2010, Lago and Sullivan 2011) or steel racks (Krawinkler *et al.* 1979) up to possibly 10% or more for masonry (Magenes *et al.* 2008) or timber partitions (Filiatrault *et al.* 2004) and therefore spectra should be capable of accounting for the likely damping level.

The importance of the damping ratio of non-structural elements in regards to the construction of floor response spectra can be explained with reference to concepts related to dynamic amplification of structures subject to harmonic loading. The earthquake excitation of a building will excite its various modes of vibration. Consequently, one could expect the accelerations at the roof level of an SDOF system to vary harmonically at a frequency corresponding to the natural frequency of the supporting structure. As is demonstrated in many texts on the dynamics of structures (e.g. Thomsen and Dahleh 1998, Chopra 2000), the acceleration response of a SDOF system subjected to harmonic forces can be calculated as the "static" acceleration multiplied by a dynamic amplification factor, DAF_a. At resonance (i.e. when the forcing frequency corresponds to the natural frequency of the structure), the DAF_a reaches its peak, the value of which is limited only by the damping ratio, ξ, of the structure ($DAF_a = 1/2\xi$).

As discussed by Sullivan et al. (2013), the expression derived for harmonic loads is too conservative for structures subject to seismic shaking since earthquakes do not impose harmonic excitation of infinite duration. However, the concept of "apparent dynamic amplification" was introduced in the context of the construction of floor spectra. The apparent dynamic amplification factors are intended as the peak spectral acceleration divided by the peak acceleration of the supporting structure (obtained for example from NLTH analyses).

The apparent dynamic amplification coefficient for use in the construction of floor response spectra could be considered a function of the following three parameters:

(1) the ratio of the period of vibration of the supporting structure to the period of vibration of the supported element;

(2) the duration of the seismic excitation (or better, the number of forcing cycles); and

(3) the "regularity", in terms of amplitude, of the seismic excitation itself.

Both the duration (or number of forcing cycles) and the average amplitude of the equivalent forcing function are difficult to define for seismic conditions since they are likely to be sensitive to the ground motion characteristics and characteristics of the supporting structure. Such difficulties help explain why none of the international seismic codes propose the same approach for estimating floor spectra and instead incorporate empirical procedures.

3.2 Effects of non-linearity of the supporting structure

Floor accelerations, and more generally the seismic actions that are transferred to the non-structural elements attached to the various levels of a building, are inevitably affected by the building response. More specifically, different non-structural demands should be expected if the supporting structure responds elastically or not.

The floor spectral peak acceleration, which could be expressed as the peak floor acceleration multiplied by an appropriate dynamic amplification factor, would be expected to occur when the period of the supported element corresponds to the period of vibration of the supporting structure.

Prior to activation, friction base isolators have an almost perfectly rigid lateral stiffness. In this context, a structure's dynamic properties correspond to those of a fixed-base system. Periods of vibrations and mode shapes can be calculated as for linear MDOF systems, in line with classic approaches. After activation, the effective stiffness of the isolator, and in turn that of the whole structure, inevitably decreases. The effective period of the structure elongates proportionally to a stiffness value that ranges from the post activation stiffness to a secant stiffness at maximum displacement.

Consequently, because the period of the supporting structure lengthens during the seismic response it is clear that the apparent forcing period on the supported elements should also be expected to lengthen by the same amount. As such, the maximum acceleration could be expected to occur over the period range from the initial fundamental period of the structure through to the effective period of the structure (associated for example with the secant stiffness at peak response).

Therefore, when the supporting structure responds inelastically there is a tendency for an acceleration plateau to develop in the floor spectra. This plateau is more evident in SDOF supporting structures, but it can be observed in Fig. 5 as well with reference to the fundamental mode of the structure (i.e. the highest elastic period).

It should be noted that the larger the ductility demand on the supporting structure, the wider the plateau tends to be. Note that when a SDOF supporting structure yields (or activates, in case of friction base isolators) and non-linear response develops, the maximum acceleration of the floor grows somewhat slowly, being a function of the force-displacement relationship characterizing the system and being proportional to the maximum displacement experienced. More details on this can be found in Menon and Magenes (2008) and Sullivan et al. (2013). This phenomenon is illustrated schematically in Fig. 6.

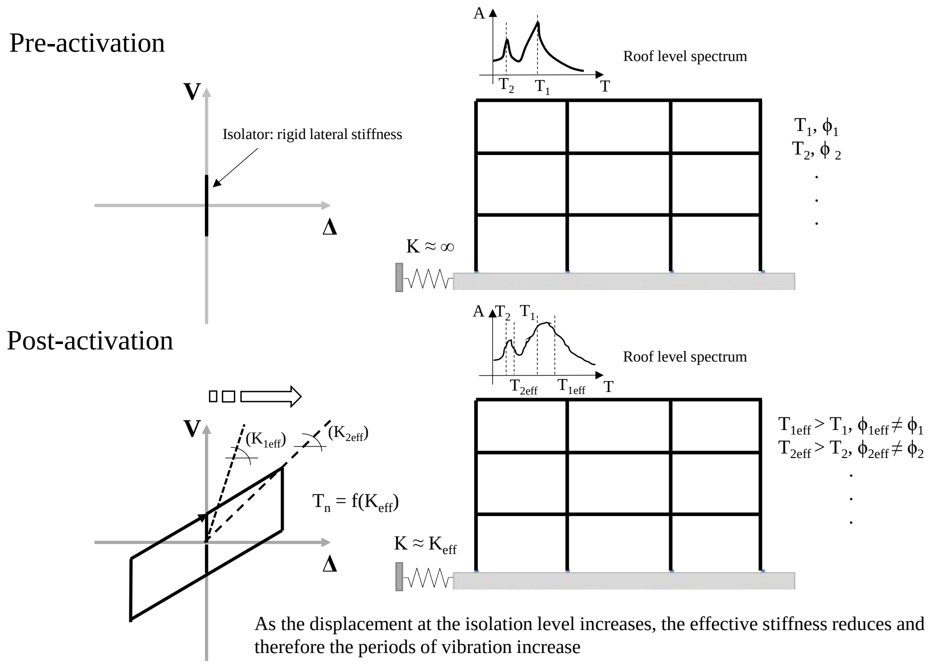

Fig. 6 – Force-displacement response of a Friction Pendulum, annotated to illustrate concept pre- and post-activation effective stiffness and effective periods at different displacement levels.

3.3 Effects of higher modes

Even though the contributions of higher modes can often be neglected from the point of view of displacements, the floor accelerations that are produced by higher modes of vibration can be very significant. Calvi and Sullivan (2014) showed that the higher modes (the second mode, in particular) can produce large floor acceleration spikes, even in a simple 2DOF regular elastic system. The contributions of higher modes influence the shape and the intensity of floor response spectra significantly. As a consequence, neglecting the effects of the higher modes of vibration when constructing acceleration response spectra at different levels of a building can lead to inaccurate evaluation of the risks associated with components characterized by low periods.

It is evident from the results shown in Fig. 5 that the effects of the higher modes remain significant even in base isolated structures. Acceleration spikes can be observed at values at or slightly higher than the second and third elastic periods of vibration.

To this end, it is important to discuss the effects that base isolation have on the acceleration response of a MDOF system and on how base isolation affects the higher modes of the structure and, consequently, the floor response spectra. Triggering non-linear behavior (that is, activating a base plastic mechanism such as a base isolator) has the greatest effect on the first mode of vibration of the system. Forces and accelerations associated with the first mode of vibration are normally capped by the maximum strength of the system and the effective fundamental period lengthens significantly as a function of the secant stiffness, as discussed in the previous section. However, higher modes are normally much less affected by the activation of a plastic mechanism at the base of the structure. For instance, Wiebe and Christopoulos (2009), discussed how little the higher modes in a shear wall building are influenced by the activation of a rotational plastic hinge at the base the wall.

Similarly, a base isolator installed beneath a structure has much greater effect on the seismic actions associated with the first mode of vibration than on the higher modes. Fig. 7 shows the ratio of each fundamental period in the isolated structures to the corresponding fixed-base period. The pendulum stiffness has been used for the FP devices in the isolated case. It can be seen that the first mode period is shifted considerably for all three case-study structures, while the higher modes remain essentially stationary.

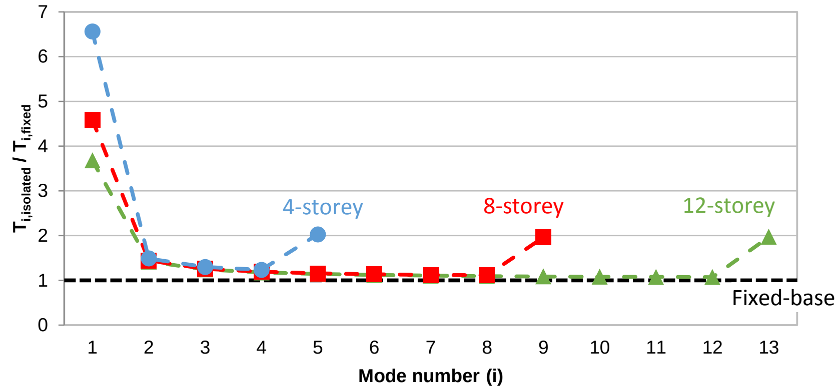

Fig. 7 – Change of period in isolated structures.

Another important aspect that emerges from the numerical analyses and that can, to some extent, be attributed to the effects of the higher modes, concerns the accelerations recorded at the ground floor of the base isolated structures. In most cases, the peak accelerations at the ground floor slab are found to be higher than the peak ground acceleration. This is illustrated with an example of the time history results in Fig. 8. It is shown in Fig. 5 that the "ground floor" response spectra are also distinctly different from the ground response spectra used for the design of the main system. This is a consequence of the ground floor accelerations being significantly different from the ground acceleration on account of the filtering action provided by the isolation layer.

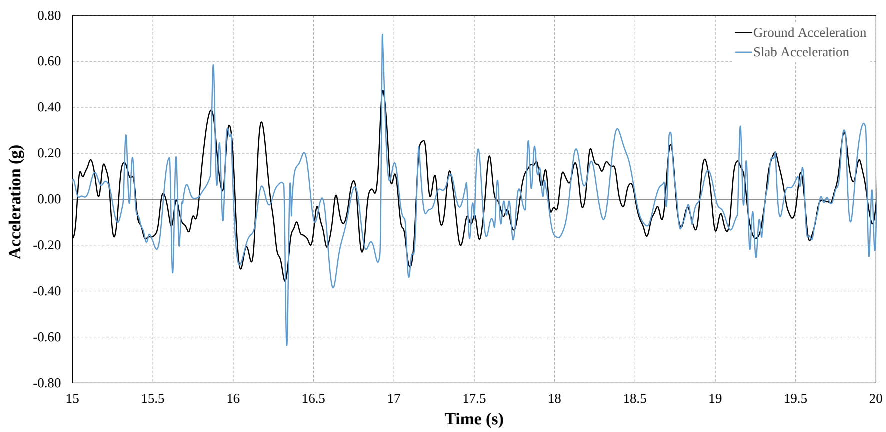

Fig. 8 – Comparison of ground acceleration and acceleration recorded at the slab for the 8 storeys case study structure subjected to earthquake EQ1.

Wiebe and Christopoulos (2010) investigated acceleration spikes in rocking shear wall systems and concluded that the observed spikes were partially due to physical phenomenon but partially due to modeling assumptions. In particular, the idealization of flag-shape hysteresis as simple linear piece-wise with sharp corners in correspondence of stiffness changes was the cause of some artificially high acceleration values.
It was shown (Wiebe and Chrisopoulos 2011) that the use hysteresis with round in place of sharp corners could lead to more realistic estimates of the floor accelerations in rocking shear wall systems. No specific guidance pertaining to base isolated systems was provided. It is reasonable to expect that the spikes observed in this study may be partly physical and partly the result of modeling decisions. However, unlike self-centering rocking hystereses which are characterized by somewhat rounded corners in real systems, force-displacement relationships for real friction isolators do have abrupt changes in stiffness, so the idealization is reasonable.
It is evident that this should be an area of further research and that, in all cases, particular care should go into designing the non-structural elements located at the ground floor of isolated structures, since the seismic demand for these elements could, counterintuitively, be higher than it is in non-isolated systems.

4. Conclusions

This paper has shown that earthquake-induced floor accelerations in base isolated structures can be significant and that predicting floor response spectra is a non-trivial problem that has thus far received little attention. Current code provisions were formulated specifically to construct floor spectra for structures with fixed bases and have been shown to be unsuitable for application to base isolated systems. To this end, the results of the numerical analyses conducted have shown that the non-structural demand in base isolated structures is influenced by a number of parameters such as the damping of the non-structural elements and the non-linearity and the higher modes of the main structure. This preliminary work has focused on structures isolated by means of Friction Pendulum devices, but the findings can be generalized to any other base isolation system.

Further research should be conducted to provide enough data to support the formulation of reliable methodologies to estimate the non-structural seismic demand in base isolated systems.

5. Copyrights

6. References

[1] FEMA 366 (2008): HAZUS-MH Estimated Annualized Earthquake Losses for the United States, Washington, DC.

[2] Dhakal RP (2010): Damage to non-structural components and contents in the 2010 Darfield earthquake. *B. Earthq. Eng.*, **43**(4), 404-411.

[3] Villaverde R (1997): Seismic design of secondary structures: state of the art. *J. Struct. Eng.-ASCE*, **123**(8), 1011-1019.

[4] The New Zealand Treasury (2011): Budget economic and fiscal update 2011. ISBN: 978-0-478-37812-2 (Online) http://purl.oclc.org/nzt/b-1381.

[5] Filiatrault A, Sullivan TJ (2014): Performance-based seismic design of nonstructural building components: The next frontier of earthquake engineering. *Earthquake Engineering and Engineering Vibration*, **13**(1), 17-46.

[6] Warn GP, Ryan KL (2012): A review of seismic isolation for buildings: historical development and research needs: *Buildings 2*: pp. 300–325.

[7] Ryan KL, Dao ND, Sato E, Sasaki T, Okazaki T (2012): Aspects of isolation device behavior observed from full-scale testing of an isolated building at E-defense: *Proceedings of the 20th Analysis and Computation Specialty Track* (2012 ASCE Structures Congress), Chicago, IL, USA.

[8] Priestley MJN, Calvi GM, Kowalsky MJ (2007): *Direct displacement-based seismic design*. IUSS Press, Pavia, Italy.

[9] Chopra AK (2000): *Dynamics of structures*. Pearson Education, USA.

[10] Jacobsen LS (1960): Damping in Composite Structures. *2nd World Conference on Earthquake Engineering*, Tokyo and Kyoto, Japan.

[11] MATLAB and Statistics Toolbox Release 2012, The MathWorks, Inc., Natick, MA

[12] Newmark NM, Rosenblueth E (1971): *Fundamentals of Earthquake Engineerin.* Prentice Hall, Englewood Cliffs, NJ.

[13] Petrini L, Maggi C, Priestley MJN, Calvi GM (2008): Experimental verification of viscous damping modeling for inelastic time history analyses. *Journal of Earthquake Engineering*, **12**(1), 125-145.

[14] Smyrou E, Priestley NMJ, Carr AJ (2011): Modelling of elastic damping in nonlinear time history analyses of cantilever RC walls. Bull Earthquake Engineering, **9**(5), 1559-1578.

[15] Hall JF (2006): Problems encountered from the use (or misuse) of Rayleigh damping. *Earthquake Eng. Struct. Dyn.*, **35**(5), 525–545.

[16] Ryan KL, Polanco J (2008): Problems with Rayleigh Damping in Base-Isolated Buildings. *J. Struct. Eng.*, **134**(11), 1780-1784.

[17] Fagà E (2013): A precast composite technology for seismic design of multi-storey buildings. Istituto Universitario di Studi Superiori di Pavia - IUSS.

[18] CEN EC8 (2004): Eurocode 8 – Design provisions for earthquake resistant structures, EN-1998-1:2004: E, Comite Europeen de Normalization, Brussels, Belgium.

[19] ASCE/SEI 7-05 (2005): Minimum design loads for buildings and other structures, American Society of Civil Engineers, 388.

[20] Nakagami Y. (2003): Probabilistic dynamics of wind excitation on glass façade. *Doctoral Thesis*, University of Darmastadt, Germany.

[21] Lenk P, Coult G (2010): Damping of glass structures and components. *2nd Challenging Glass Conference*, Delft, The Netherlands.

[22] Lago A, Sullivan TJ (2011): A review of glass façade systems and research into the seismic design of frameless glass façades. *IUSS Research Report* No. ROSE-2011/01, IUSS press, Pavia.

[23] Krawinkler H, Cofie NG, Astiz MA, Kircher CA (1979): Experimental study on the seismic behaviour of industrial storage racks. *Report 41*, John A. Blume Earthquake Engineering Center, Stanford University, California.

[24] Magenes G, Morandi P, Penna A (2008): Experimental in-plane cyclic response of masonry walls with clay units. 14th World Conference on Earthquake Engineering, Beijing, China.

[25] Filiatrault A, Epperson M, Folz B (2004): Equivalent elastic modelling for the direct displacement based seismic design of wood structures. *ISET J. Earthq. Technol.*, **41**(1), 75-99.

[26] Thomson WT, Dahleh MD (1998): *Theory of vibration with applications*. Prentice Hall, 5th Edition.

[27] Sullivan TJ, Calvi PM, Nascimbene R (2013): Towards Improved Floor Spectra Estimates for Seismic Design, *Earthquakes and Structures Journal*, **4**(1), 109-132.

[28] Menon A, Magenes G (2008): Out-of-plane seismic response of unreinforced masonry definition of seismic input. *Research Report ROSE – 2008/04*, IUSS Press, Pavia, Italy.

[29] Calvi PM, Sullivan TJ (2014): Estimating floor spectra in multiple degree of freedom systems, *Earthquake and Structures Journal*, **7**(1), 17-38.

[30] Wiebe L, Christopoulos C (2009): Mitigation of higher mode effects in base-rocking systems by using multiple rocking sections, *Journal of Earthquake Engineering*, **13**(1), 83-108.

[31] Wiebe L, Christopoulos C (2010): Characterizing acceleration spikes due to stiffness changes in nonlinear systems, *Earthquake Engineering and Structural Dynamics*, **39**(14), 1653-1670.

[32] Wiebe L, Christopoulos C (2011): Using Bézier curves to model gradual stiffness transitions in nonlinear elements: Application to self-centering systems, *Earthquake Engineering and Structural Dynamics*, **40**(14), 1535-1552.